

Probing the inverse moment of B_s -meson distribution amplitude via $B_s \rightarrow \eta_s$ form factors

Rusa Mandal¹, Praveen S Patil² and Ipsita Ray³

*Indian Institute of Technology Gandhinagar, Department of Physics,
Gujarat 382355, India*

Abstract

We investigate the inverse moment of the B_s -meson light-cone distribution amplitude (LCDA), denoted as λ_{B_s} and defined within the heavy quark effective theory, through the calculation of $B_s \rightarrow \eta_s$ form factors. The presence of the s -quark inside the B_s -meson dictates a notable departure of approximately 20% in the λ_{B_s} value compared to the non-strange case λ_{B_q} , as computed within the QCD sum rule approach, albeit with significant uncertainty. First, we compute the decay constant of the η_s -meson utilizing two-point sum rules while retaining finite s -quark mass contributions. Next, we constrain the parameter λ_{B_s} by calculating $B_s \rightarrow \eta_s$ form factors within the light-cone sum rule approach, using B_s -meson LCDAs, and leveraging Lattice QCD estimates at zero momentum transfer from the HPQCD collaboration. Our findings yield $\lambda_{B_s} = 480 \pm 92$ MeV when expressing the B_s -meson LCDAs in the Exponential model, consistent with previous QCD sum rule estimate yet exhibiting a 1.5-fold improvement in uncertainty. Furthermore, we compare the form factor predictions, based on the extracted λ_{B_s} value, with earlier analyses for other channels such as $B_s \rightarrow D_s$ and $B_s \rightarrow K$.

¹Email: rusa.mandal@iitgn.ac.in

²Email: praveen.patil@iitgn.ac.in

³Email: ipsita.r@iitgn.ac.in

1 Introduction

The difference between the light quark masses and strange quark mass leads to the violation of $SU(3)_F$ symmetry. This has influenced various observations in the hadron data from the early days. The difference between the properties of $B_{u,d}$ and B_s -meson is one such example. For instance, the ratio $f_{B_s}/f_{B_{u,d}}$ computed from Lattice QCD exhibits a deviation of approximately 20% from unity. Another crucial aspect of mesons lies in their internal non-perturbative structure, characterized by light-cone distribution amplitudes (LCDAs). These enter in the theory prediction of exclusive decays computed within certain approaches such as QCD factorization and heavy-quark expansion. The inverse moment of the leading twist distribution amplitude, λ_{B_q} , is the key parameter to model the behaviour of all the LCDAs.

The estimate of λ_{B_q} is available within the framework of QCD sum rules which suffers from significantly large uncertainty [1]. The first attempt to compute the inverse moment for B_s -meson LCDA namely, λ_{B_s} , can be found in Ref. [2] where the effect of finite s -quark mass and difference between strange and non-strange quark condensate densities are systematically considered. In this study, the individual estimate was determined to be $\lambda_{B_s} = 438 \pm 150$ MeV, with the ratio $\lambda_{B_s}/\lambda_{B_q} = 1.19 \pm 0.14$ demonstrating a 20% departure from unity, indicative of $SU(3)_F$ violation¹. While in the future, accurate measurement of the photoleptonic mode $B \rightarrow \ell\nu\gamma$ will be able to provide better estimate of the parameter λ_{B_q} under the well-established factorization framework, the prospect for λ_{B_s} is not promising in this regard as the corresponding channel for B_s , i.e., $B_s \rightarrow \ell\ell\gamma$ is prone to non-local contributions [4] that may contaminate the extraction of λ_{B_s} . Although one feasible approach involves utilizing the same inverse moment for non-strange and strange B -mesons in theoretical predictions while disregarding $SU(3)_F$ violation effects, this may lead to erroneous conclusions when comparing with the burgeoning dataset of B_s -meson decay modes in recent years. Consequently, there is a timely need to explore alternative methods to mitigate the uncertainty associated with the parameter λ_{B_s} .

In this work, we utilize inputs from Lattice QCD regarding the η_s -meson, a hypothetical $s\bar{s}$ state, whose mass is determined in terms of pion and kaon masses. This configuration is more cost-effective to simulate on the lattice and is employed to calibrate the s -quark mass in analyses involving strange mesons. The mass and decay constant values are reported as $m_{\eta_s} = 0.6885(22)$ GeV and $f_{\eta_s} = 0.181(55)$ GeV, respectively [5]. We can regard this $s\bar{s}$ contribution as one component of the familiar $\eta - \eta'$ states, where the other component consists of light quarks². Notably, using data on the η_s state enables us to extract pertinent information bypassing the complexities associated with octet-singlet mixing parameterization.

Recently, the HPQCD collaboration [7] has provided form factor estimates of several B to light-meson states at the maximum recoil of the light-meson with greater accuracy. The results are then used in Ref. [8] to provide indirect extraction of λ_{B_q} using light-cone sum rule (LCSR) framework where a notable two times improvement in the uncertainty is obtained. In similar spirit, here we compute the $B_s \rightarrow \eta_s$ form factors within LCSR approach and analyse the Lattice estimates to constrain the parameter λ_{B_s} . To the best of our knowledge, this represents the first indirect determination of the inverse moment of the leading twist B_s -meson LCDA.

The paper is organized as follows. We first compute the two-point sum rules for the η_s -meson

¹The finite s -quark mass effects in the general B_s -meson LCDA parametrization have recently been investigated in Ref. [3] offering QCD sum rule compatible values for λ_{B_s} within certain range of the model parameters.

²For previous study on B_s -meson to $\eta - \eta'$ form factor calculated using QCD sum rule method see Ref. [6].

decay constant in the QCD sum rule framework in Sec. 2. The prediction for decay constant with the inputs used are also provided there. In Sec. 3, we first briefly outline the computation of $B_s \rightarrow P$ form factors, where P is any pseudoscalar meson, using B_s -meson LCDAs. We present the result on λ_{B_s} extraction and compare the form factor predictions for several decay modes in Sec. 4. Finally in Sec. 5 we summarize the outcomes. Several appendices contain the useful expressions e.g., LCDA parametrization in Appendix A, coefficients of the LCSRs for form factors in Appendix B and correlation matrices of the fitted coefficients in Appendix C obtained in this analysis for the $B_s \rightarrow P$ form factors.

2 Two-point sum rule for decay constant

In this section, we start by computing the two-point sum rule for the decay constant of the η_s -meson. Subsequently, we conduct a numerical analysis to provide an estimate for the decay constant. The ranges determined for certain input parameters, such as the effective threshold and Borel parameter, may be applied in the following section, where we calculate the form factors for the $B_s \rightarrow \eta_s$ transition. The two-point correlation function of the axial-vector current $J_\mu = \bar{s}\gamma_\mu\gamma_5 s$ reads

$$\begin{aligned}\Pi_{\mu\nu}(q^2) &= i \int d^4x e^{iqx} \langle 0 | \mathcal{T} \{ J_\mu(x) J_\nu^\dagger(0) \} | 0 \rangle \\ &= (-g_{\mu\nu}q^2 + q_\mu q_\nu) \Pi_T(q^2) + q_\mu q_\nu \Pi_L(q^2),\end{aligned}\tag{1}$$

where in the second line the correlation function is decomposed into two tensor structures whose coefficients are Lorentz invariant amplitudes Π_T and Π_L . The partial conservation of axial current dictates that pseudoscalar mesons contribute to Π_L amplitude while axial-vector meson contributions are encoded in Π_T . Hence as η_s is a pseudoscalar meson, contribution from the pseudoscalar states can be isolated by projecting out the correlation function as

$$q^2 \Pi_L(q^2) = \frac{q^\mu q^\nu}{q^2} \Pi_{\mu\nu} \equiv \hat{\Pi}(q^2).\tag{2}$$

For the rest of our analysis, we only focus on the $\hat{\Pi}$ part of the correlation function.

In order to derive the hadronic spectrum of the correlation function (1), we presume the lowest lying state is the pseudoscalar ($J^P = 0^-$) i.e. η_s -meson. The hadronic dispersion relation for the two-point function can be written as

$$\hat{\Pi}_{\text{had}}(q^2) = \int_0^\infty ds \frac{\rho_{\text{had}}(s)}{s - q^2},\tag{3}$$

where $\rho_{\text{had}}(s)$ denotes the hadronic spectral density $\rho_{\text{had}}(s) = \frac{1}{\pi} \text{Im} \hat{\Pi}_{\text{had}}(s)$. Defining the decay constant f_{η_s} for η_s -meson as

$$\langle 0 | \bar{s}\gamma_\mu\gamma_5 s | \eta_s(k) \rangle = i k_\mu f_{\eta_s},\tag{4}$$

we write

$$\rho_{\text{had}}(s) = m_{\eta_s}^2 f_{\eta_s}^2 \delta(s - m_{\eta_s}^2) + \rho_{\text{cont}}(s) \Theta(s - s_{th}),\tag{5}$$

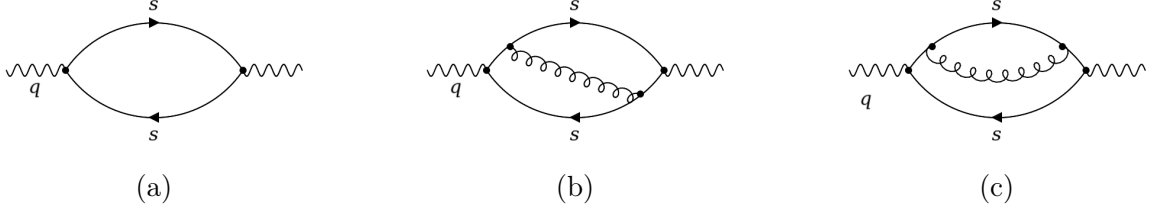


Figure 1: Diagrams representing the perturbative part of the correlation function: (a) quark loop at leading order, (b) – (c) the gluon radiative corrections at NLO ($\mathcal{O}(\alpha_s)$).

where the ρ_{cont} denotes the higher excited and continuum states, and s_{th} the lowest threshold of the states heavier than η_s -meson. We then substitute the spectral density into the dispersion relation (3) and perform a Borel Transformation to remove the subtraction terms³ and obtain exponentially suppressed contribution from ρ_{cont} .

$$\hat{\Pi}_{\text{had}} = f_{\eta_s}^2 m_{\eta_s}^2 e^{-m_{\eta_s}^2/M^2} + \int_{s_{th}}^{\infty} ds e^{-s/M^2} \rho_{\text{cont}}(s), \quad (6)$$

where M^2 is the Borel parameter.

Next we proceed to compute the local operator product expansion (OPE) of the correlator (1) which can be decomposed in two parts. The leading effect of this expansion gives the perturbative contribution and the higher order terms are given by a series of QCD vacuum condensates multiplied by the corresponding Wilson coefficients.

$$\hat{\Pi}_{\text{OPE}}(q^2) = \hat{\Pi}_{\text{pert}}(q^2) + \hat{\Pi}_{\text{cond}}(q^2). \quad (7)$$

The spectral density of the correlator $\hat{\Pi}_{\text{pert}}(q^2)$ is defined as $\rho_{\text{pert}}(s) = \frac{1}{\pi} \text{Im} \hat{\Pi}_{\text{pert}}(s)$, and at leading order in α_s , Fig. 1a is

$$\rho_{\text{pert}}^{\text{LO}}(s) = \frac{3m_s^2}{2\pi^2} \frac{\sqrt{s(s-4m_s^2)}}{s}. \quad (8)$$

The next-to-leading order (NLO) contribution to the perturbative spectral density $\rho_{\text{pert}}^{\text{NLO}}$ has been performed in Ref. [9] for both vector and axial vector quark currents by retaining two distinct masses for the quarks. We use the expression with the suitable substitution for same quark masses. The corresponding diagrams are shown in Figs. 1b and 1c.

The QCD vacuum condensates are organized in series with increasing mass dimension of the respective operators. We consider contributions up to $d = 5$ condensates,

$$\hat{\Pi}_{\text{cond}} = \hat{\Pi}^{\langle \bar{q}q \rangle} + \hat{\Pi}^{\langle GG \rangle} + \hat{\Pi}^{\langle \bar{q}Gq \rangle}, \quad (9)$$

where $\hat{\Pi}^{\langle \bar{q}q \rangle}$, $\hat{\Pi}^{\langle GG \rangle}$ and $\hat{\Pi}^{\langle \bar{q}Gq \rangle}$ are the quark, gluon and quark-gluon condensate contributions, respectively. The lowest condensate contribution is at $d = 3$ which is attributed to the case

³For our choice of the current in (1), one subtraction $\hat{\Pi}(0)$ is sufficient for the convergence of the integral in the dispersion relation (3).

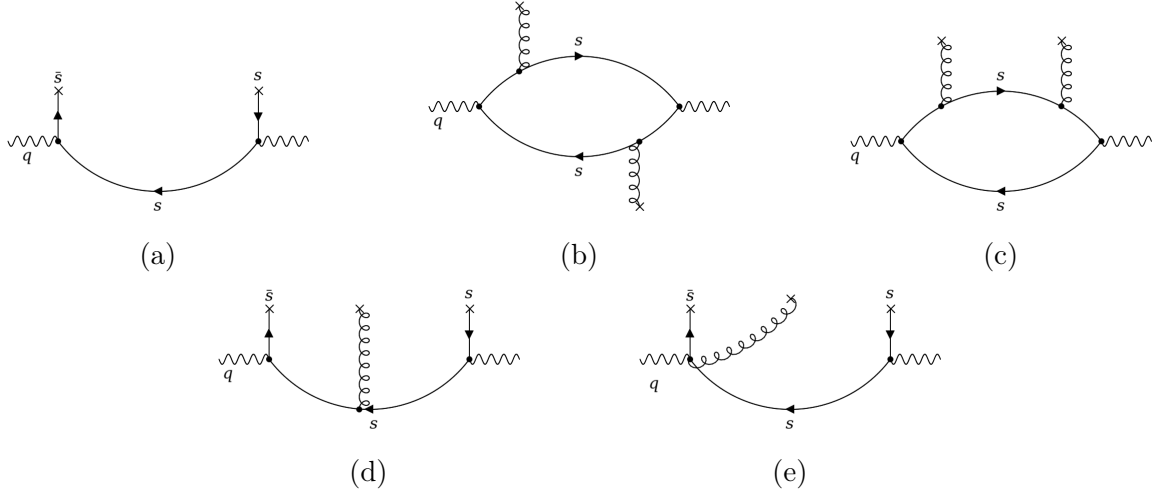


Figure 2: Various contributions to the condensate terms: (a) $s\bar{s}$ quark condensate, (b) – (c) gluon condensate and (d) – (e) quark-gluon condensate contributions. Crossed lines denote vacuum fields.

where one of the s -quark propagates perturbatively and the other one is absorbed and emitted by the s -quark condensate term, as shown in Fig. 2a. Expanding the quark fields as

$$s(x) = s(0) + x^\mu \vec{D}_\mu s(0) + \frac{1}{2} x^\mu x^\nu \vec{D}_\mu \vec{D}_\nu s(0) + \dots, \quad (10)$$

and taking the second term in the expansion, we obtain

$$\hat{\Pi}^{(\bar{q}q)}(q^2) = m_s \left(\frac{3}{q^2 - m_s^2} + \frac{q^2}{(q^2 - m_s^2)^2} \right) \langle \bar{s}s \rangle. \quad (11)$$

Next arises the $d = 4$ gluon condensate contributions in which we consider both the diagrams namely, one gluon emission from each of the two quark propagators, Fig. 2b and two gluon emission from either of the quarks, Fig. 2c. The resultant contribution to the correlator is [10]

$$\hat{\Pi}^{(GG)}(q^2) = \left(-\frac{1}{12m_s^2} - \frac{m_s^2}{4(-4m_s^2 + q^2)^2} - \frac{5}{24(-4m_s^2 + q^2)} \right) \langle GG \rangle. \quad (12)$$

Interestingly, apart from the contribution in Eq. (12), we also generate imaginary contribution due to the presence of logarithms, which can be added to the OPE using dispersion relation (similar to the contribution to the perturbative part) of the following form.

$$\hat{\Pi}^{(GG)}(q^2) = \langle GG \rangle \int_{4m_s^2}^{\infty} \frac{ds}{s - q^2} \rho^{(GG)}(s), \quad (13)$$

where

$$\rho^{(GG)}(s) = \frac{-30m_s^6 + 7m_s^4 s + m_s^2 s^2}{2s^4}. \quad (14)$$

We then take into account the effect of propagating quarks with quark-gluon condensate, where the vacuum expectation value of the quark-gluon-quark operator can be parametrized in terms of the parameter m_0 defined as

$$\langle 0 | \bar{q} g_s G_{\mu\nu}^a t^a \sigma^{\mu\nu} q | 0 \rangle = \langle \bar{q} G q \rangle = m_0^2 \langle \bar{q} q \rangle. \quad (15)$$

In this scenario, the contribution arises from two distinct effects; firstly, when the gluon emitted from the quark propagator ends in the vacuum, see Fig. 2d. Secondly, it stems from the term involving two covariant derivatives in the expansion of the quark field, Eq. (10). In the latter instance, the commutator of two covariant derivatives is proportional to the gluon field strength, which, upon combining with quark and anti-quark fields, forms the condensate. This can be interpreted as a gluon originating from the vacuum quark or anti-quark line, see Fig. 2e. Summing these two effects, the resultant contribution is

$$\hat{\Pi}^{\langle\bar{q}Gq\rangle}(q^2) = \frac{1}{2} \frac{m_s^3}{(m_s^2 - q^2)^3} m_0^2 \langle\bar{s}s\rangle. \quad (16)$$

After performing Borel Transformation in the variable q^2 of both the perturbative and condensate parts of the OPE, the correlation function is given by

$$\begin{aligned} \hat{\Pi}_{\text{OPE}} = & \int_{4m_s^2}^{\infty} ds e^{-s/M^2} \left[\rho_{\text{pert}}^{\text{LO}}(s) + \frac{\alpha_s}{\pi} \rho_{\text{pert}}^{\text{NLO}}(s) + \rho^{\langle GG\rangle}(s) \langle GG\rangle \right] \\ & - 4m_s e^{-m_s^2/M^2} \left(1 - \frac{m_s^2}{4M^2} - \frac{m_s^2 m_0^2}{16M^4} \right) \langle\bar{s}s\rangle + \left(\frac{5}{24} - \frac{m_s^2}{4M^2} \right) e^{-4m_s^2/M^2} \langle GG\rangle. \end{aligned} \quad (17)$$

We are now at a stage to write down the QCD sum rules for the decay constant using the quark-hadron duality approximation. In the asymptotic region of the spacelike momentum transfer, $q^2 \rightarrow -\infty$, the correlation function (1) represents a short distance quark anti-quark fluctuation and can be treated in perturbative QCD. By making the use of Borel Transformation, which sets the momentum transferred variable q^2 to infinitely spacelike distances, the hadronic and perturbative parts of the correlation function can be made to coincide due to the absence of poles or cuts. We use semi-local quark-hadron duality assumption which dictates that the hadronic spectral density $\rho_{\text{cont}}(s)$, introduced in Eq. (5) is equal to the perturbative part above some effective threshold s_{th} , as a consequence the integral over spectral density from s_{th} to ∞ drops out while equating the OPE, Eq. (17) with the hadronic side, Eq. (6). The utilization of the Borel Transformation is crucial in this context, as it introduces an exponential suppression that reduces sensitivity to the assumption. We then obtain the sum rule for the decay constant for η_s -meson as

$$\begin{aligned} f_{\eta_s}^2 m_{\eta_s}^2 e^{-m_{\eta_s}^2/M^2} = & \int_{4m_s^2}^{s_{th}} ds e^{-s/M^2} \left[\rho_{\text{pert}}^{\text{LO}}(s) + \frac{\alpha_s}{\pi} \rho_{\text{pert}}^{\text{NLO}}(s) + \rho^{\langle GG\rangle}(s) \langle GG\rangle \right] \\ & - 4m_s e^{-m_s^2/M^2} \left(1 - \frac{m_s^2}{4M^2} - \frac{m_s^2 m_0^2}{16M^4} \right) \langle\bar{s}s\rangle + \left(\frac{5}{24} - \frac{m_s^2}{4M^2} \right) e^{-4m_s^2/M^2} \langle GG\rangle. \end{aligned} \quad (18)$$

All the input parameters that are needed for the numerical evaluation are listed in Table 1. The Borel parameter has to be chosen large enough such that the higher power correction in the OPE are sufficiently suppressed but small enough such that the contribution of continuum and excited states is subleading compared to the one of the lowest resonance. Also the sum rule should be independent of Borel parameter. These conditions are satisfied when the Borel parameter is in the range.

$$M^2 = [2, 3] \text{ GeV}^2. \quad (19)$$

| Parameter | Values | References |
|--|---|------------|
| Normalization scale | $\mu = 1.5 \text{ GeV}$ | [11, 12] |
| s -quark mass | $m_s(\mu = 1.5 \text{ GeV}) = 0.1016 \pm 0.0094 \text{ GeV}$ | [13, 14] |
| Strong coupling | $\alpha_s(\mu = 1.5 \text{ GeV}) = 0.3494 \pm 0.0092$ | [13, 14] |
| Quark condensate | $\langle \bar{q}q \rangle = (-0.278 \pm 0.022 \text{ GeV})^3$ | [15] |
| s -quark condensate | $\langle \bar{s}s \rangle / \langle \bar{q}q \rangle = (0.8 \pm 0.3)$ | [16] |
| Ratio $\langle \bar{q}Gq \rangle / \langle \bar{q}q \rangle$ | $m_0^2 = 0.8 \pm 0.2 \text{ GeV}^2$ | [16] |
| Gluon condensates | $\langle GG \rangle = 0.012 \pm 0.012 \text{ GeV}^4$ | [16] |
| η_s -meson mass | $m_{\eta_s} = 0.6885 \pm 0.0022 \text{ GeV}$ | [17] |

Table 1: The input parameters used in two-point sum rule of the η_s -meson decay constant.

The effective threshold s_{th} is determined in the following way: we take the derivative of the sum rule with respect to $-1/M^2$ and divide the result by the initial sum rule, which gives

$$m_{\eta_s}^2 = \frac{\int_{4m_s^2}^{s_{th}} ds s e^{-s/M^2} \left[\rho_{\text{pert}}^{\text{LO}}(s) + \frac{\alpha_s}{\pi} \rho_{\text{pert}}^{\text{NLO}}(s) + \rho^{\langle GG \rangle}(s) \langle GG \rangle \right] + \frac{d\hat{\Pi}_{\text{cond}}}{d\left(\frac{-1}{M^2}\right)}}{\int_{4m_s^2}^{s_{th}} ds e^{-s/M^2} \left[\rho_{\text{pert}}^{\text{LO}}(s) + \frac{\alpha_s}{\pi} \rho_{\text{pert}}^{\text{NLO}}(s) + \rho^{\langle GG \rangle}(s) \langle GG \rangle \right] + \hat{\Pi}_{\text{cond}}}. \quad (20)$$

In the Borel window mentioned above, the effective threshold s_{th} takes the value

$$s_{th} = (4.9 \pm 1.6) \text{ GeV}^2, \quad (21)$$

and evaluating the sum rule (18), yields the decay constant

$$f_{\eta_s} = (187 \pm 37) \text{ MeV}. \quad (22)$$

This value is consistent with the Lattice QCD estimate⁴ and the relation involving K -meson and pion decay constants, namely $\sqrt{2} f_K^2 - f_\pi^2$ [5].

3 Light-cone sum rules for form factors

In order to construct the LCSRs for $B_s \rightarrow \eta_s$ transition form factors, we start with the B_s -to-vacuum correlator

$$\mathcal{F}^{\mu\nu}(q, k) = i \int d^4x e^{ik \cdot x} \langle 0 | \mathcal{T} \{ J_{\text{int}}^{\nu\dagger}(x), J_{\text{weak}}^\mu(0) \} | \bar{B}_s(q+k) \rangle, \quad (23)$$

⁴as obtained by HPQCD collaboration $f_{\eta_s}^{\text{lat}} = (181 \pm 55) \text{ MeV}$.

of two quark currents. Here, $J_{weak}^\mu(0) \equiv \bar{s}(0)\Gamma_w^\mu b(0)$ is the weak current with the momentum q related to $B_s \rightarrow \eta_s$ transition. The interpolating current $J_{int}^\nu(x) \equiv \bar{s}(x)\gamma^\nu\gamma_5 s(x)$ is chosen to interpolate the η_s with the momentum k . With our four-momenta assignment, the momentum of the B_s -meson state is $q+k$, which satisfies the on-shell condition, $p^2 \equiv (q+k)^2 = m_{B_s}^2$. As a next step, we obtain the hadronic representation of the correlator (23) via the dispersion relation. Taking the imaginary part with respect to the variable $k^2 = s$ for $s > 0$ and isolating the lowest lying η_s state, it reads

$$\text{Im}_{k^2} \mathcal{F}_{\text{had}}^{\mu\nu}(q, k) = \pi \delta(s - m_{\eta_s}^2) \langle 0 | J_{int}^{\nu\dagger} | \eta_s(k) \rangle \langle \eta_s(k) | J_{weak}^\mu | \bar{B}_s(q+k) \rangle + \dots, \quad (24)$$

where the ellipsis denote contributions from other hadronic states with the same quantum numbers.

The first term in Eq. (24) represents η_s to vacuum transition and can be written in terms of the decay constant of the η_s -meson as defined in Eq. (4). The second term denotes $B_s \rightarrow \eta_s$ hadronic matrix element for the weak current. Due to the conservation of parity, the axial-vector current transition matrix element vanishes. Introducing three independent non-vanishing form factors $f_+(q^2)$, $f_0(q^2)$ and $f_T(q^2)$ for the vector and the tensor weak currents i.e., $\Gamma_w^\mu \equiv \Gamma_V^\mu = \gamma^\mu$ and $\Gamma_w^\mu \equiv \Gamma_T^\mu = \sigma^{\mu\nu} q_\nu$, respectively, the hadronic matrix element can be parameterized. These form factors are functions of the momentum transfer $q^2 = (p-k)^2$, however, here we suppress the explicit q^2 dependence for simplicity.

$$\langle \eta_s(k) | \bar{s}\gamma^\mu b | B_s(p) \rangle = \left[(p+k)^\mu - \frac{m_{B_s}^2 - m_{\eta_s}^2}{q^2} q^\mu \right] f_+ + \frac{m_{B_s}^2 - m_{\eta_s}^2}{q^2} q^\mu f_0, \quad (25)$$

$$\langle \eta_s(k) | \bar{s}\sigma^{\mu\nu} q_\nu b | B_s(p) \rangle = \frac{if_T}{m_{B_s} + m_{\eta_s}} \left[q^2 (p+k)^\mu - (m_{B_s}^2 - m_{\eta_s}^2) q^\mu \right]. \quad (26)$$

Substituting the definition of decay constant and the hadronic matrix elements Eqs. (25) and (26) for the vector and tensor currents respectively, in Eq. (24) we get,

$$\begin{aligned} \frac{1}{\pi} \text{Im}_{k^2} \mathcal{F}_{\text{had,V}}^{\mu\nu}(q, k) &= if_{\eta_s} \left[\left\{ 2k^\mu k^\nu - \frac{m_{B_s}^2 - m_{\eta_s}^2 - q^2}{q^2} q^\mu k^\nu \right\} f_+ \right. \\ &\quad \left. + \frac{m_{B_s}^2 - m_{\eta_s}^2}{q^2} q^\mu k^\nu f_0 \right] \delta(s - m_{\eta_s}^2) + \dots, \end{aligned} \quad (27)$$

$$\frac{1}{\pi} \text{Im}_{k^2} \mathcal{F}_{\text{had,T}}^{\mu\nu}(q, k) = \frac{-f_{\eta_s} f_T}{m_{B_s} + m_{\eta_s}} \left[2q^2 k^\mu k^\nu - (m_{B_s}^2 - m_{\eta_s}^2 - q^2) q^\mu k^\nu \right] \delta(s - m_{\eta_s}^2) + \dots \quad (28)$$

Decomposing in different Lorentz structures e.g., $k^\mu k^\nu$ for f_+ and f_T , separately for two weak currents, and $q^\mu k^\nu$ for f_\pm defined in Eq. (51), we can extract the contributions by substituting Eqs. (27) and (28) for the form factor ‘ F ’ in the dispersion relation

$$\mathcal{F}_{\text{had}}^{(F)}(q^2, k^2) = \frac{1}{\pi} \int_0^\infty ds \frac{\text{Im}_{k^2} \mathcal{F}_{\text{had}}^{(F)}(s, q^2)}{s - k^2}. \quad (29)$$

We now perform the OPE calculation of the same correlator (23). For $k^2 \ll m_s^2$ and $q^2 \ll (m_b + m_s)^2$, implying far below the hadronic thresholds in the channels of the interpolating and

weak currents, the correlator (23) can be calculated, expanding the time-ordered product of currents near the light-cone $x^2 \simeq 0$ as

$$\mathcal{F}_{\text{OPE}}^{\mu\nu}(q, k) = \int d^4x e^{ik \cdot x} \int \frac{d^4l}{(2\pi)^4} e^{-il \cdot x} [\gamma^\nu \gamma_5 \frac{\not{l} + m_s}{m_s^2 - l^2} \Gamma_w^\mu]_{\alpha\beta} \times \langle 0 | \bar{s}^\alpha(x) b^\beta(0) | \bar{B}_s(q+k) \rangle, \quad (30)$$

where α, β are spinor indices. Here the virtual s -quark propagates between the two vertices of currents, $J_{int}^{\nu\dagger}(x)$ and $J_{weak}^\mu(0)$, whereas a quark-antiquark pair emitted at a light-cone separation forms a B_s -meson state. We neglect the effect of soft-gluon emitted from the light-cone expansion of the s -quark propagator and absorbed, together with the quark-antiquark pair generating quark-antiquark-gluon (three-particle) components of the B_s -meson DAs. These effects are found to be negligible, in comparison to the two-particle contributions, for several B to light-meson transition form factors [18]. The non-local B -to-vacuum matrix element $\langle 0 | \bar{s}^\alpha(x) b^\beta(0) | \bar{B}_s(q+k) \rangle$ then can be approximated in terms of the two-particle B_s -meson LCDAs defined in the heavy quark effective theory, see Appendix A for the details. The inverse moment of the leading twist LCDA of the B_s -meson, defined as

$$\lambda_{B_s} = \left(\int_0^\infty dw \frac{\phi_+(w)}{w} \right)^{-1}, \quad (31)$$

is the key parameter in parameterizing the LCDAs. The LCDAs of higher twist also depend on the parameters λ_E and λ_H which correspond to local matrix elements denoting quark-gluon three-body components in the B_s -meson wavefunction. These differ from the three-particle components of the LCDAs which occur in vacuum to meson matrix elements including non-local quark operators. The renormalisation scale dependence of the LCDAs are neglected here and in the next section we determine the value of λ_{B_s} at a reference scale $\mu = 1 \text{ GeV}$.

Evaluating the integral in Eq. (30), after some redefinition of variables we can isolate the contribution for different form factors using the appropriate Lorentz structures as mentioned previously for the hadronic part,

$$\mathcal{F}_{\text{OPE}}^{(F)}(q^2, k^2) = f_{B_s} m_{B_s} \sum_{n=1}^4 \int_0^\infty d\sigma \frac{I_n^{(F)}(\sigma, q^2)}{(k^2 - s)^n}, \quad (32)$$

where

$$\sigma = \frac{\omega}{m_{B_s}}, \quad s(\sigma, q^2) = \sigma m_{B_s}^2 + \frac{m_s^2 - \sigma q^2}{\bar{\sigma}}, \quad \bar{\sigma} = 1 - \sigma. \quad (33)$$

The functions $I_n^{(F)}$ are combinations of two-particle LCDAs ϕ_+, ϕ_-, g_+ and g_- with twist two, three, four, and five, respectively, given as

$$I_n^{(F, 2p)}(\sigma, q^2) = \frac{1}{\bar{\sigma}^n} \sum_{\psi_{2p}} C_n^{(F, \psi_{2p})}(\sigma, q^2) \psi_{2p}(\sigma m_{B_s}), \quad \psi_{2p} = \phi_+, \bar{\phi}, g_+, \bar{g}; \quad (34)$$

with

$$\bar{\phi}(w) = \int_0^w d\eta (\phi_+(\eta) - \phi_-(\eta)), \quad \bar{g}(w) = \int_0^w d\eta (g_+(\eta) - g_-(\eta)). \quad (35)$$

The expressions for the coefficients are collected in Appendix B.

We are now at a stage to finally write the sum rules for all the form factors F by equating the OPE correlation function (32) to the hadronic representation in Eq. (29) with the assumption of semi-local quark-hadron duality. This can be written in a compact form [18],

$$F = \frac{f_{B_s} M_{B_s}}{K^{(F)}} \sum_{n=1}^4 \left\{ (-1)^n \int_0^{\sigma_0} d\sigma e^{(-s(\sigma, q^2) + m_{\eta_s}^2)/M^2} \frac{1}{(n-1)!(M^2)^{n-1}} I_n^{(F)} - \left[\frac{(-1)^{n-1}}{(n-1)!} e^{(-s(\sigma, q^2) + m_{\eta_s}^2)/M^2} \sum_{j=1}^{n-1} \frac{1}{(M^2)^{n-j-1}} \frac{1}{s'} \left(\frac{d}{d\sigma} \frac{1}{s'} \right)^{j-1} I_n^{(F)} \right]_{\sigma=\sigma_0} \right\}, \quad (36)$$

where

$$s'(\sigma, q^2) = \frac{ds(\sigma, q^2)}{d\sigma}, \quad (37)$$

and $K^{(F)}$ are normalization factors, given in the appendix in Eq. (55). In the above expression of form factors in Eq. (36), we performed the Borel transform in variable $k^2 \rightarrow M^2$. In the numerical section, the Borel window will be chosen such that the contributions from excited resonances and continuum states are exponentially suppressed and also the impact of higher-twist contributions, which varies as powers of $1/M^2$ are suppressed. Here, $\sigma_0 = \sigma(s_0, q^2)$ where s_0 is the effective threshold which is expected to be close to the mass square of the first excited state.

4 Numerical analysis and λ_{B_s} extraction

In this section, at the first part, we perform the numerical analysis to estimate the form factors using the sum rules obtained in the last section and then in the second part, we make use of the Lattice QCD inputs to determine the parameter λ_{B_s} . As already discussed in Sec. 3, the choice of the Borel parameter is an important concern in the calculation of the sum rules for the form factors. We have checked that those conditions are satisfied if we take $M^2 = [2, 3] \text{ GeV}^2$ for the $B_s \rightarrow \eta_s$ channel. To obtain the threshold parameter s_0 , we follow the similar procedure described as of the two point sum rule for the decay constant. We take the derivative of the sum rule in Eq. 36 for each form factor multiplied with $e^{-m_{\eta_s}^2/M^2}$ with respect to $-1/M^2$ and normalize it to the original sum rule. The result is equal to the mass square of the final state meson i.e.,

$$m_{\eta_s}^2 = \frac{\frac{d}{d[-1/M^2]} [F e^{-m_{\eta_s}^2/M^2}]}{F e^{-m_{\eta_s}^2/M^2}}. \quad (38)$$

In order to estimate the threshold parameter, we first quote the other inputs which enter in the form factor expressions via the B_s -meson LCDAs. The value for λ_{B_s} has been taken from Ref. [2] and those of λ_E^2 and λ_H^2 are taken from Ref. [19]. We form a multinormal distribution by varying these parameters, which follow a Gaussian distribution, within the ranges as given below.

$$\lambda_{B_s} = 0.438 \pm 0.150 \text{ GeV}, \quad \lambda_E^2 = 0.03 \pm 0.02 \text{ GeV}^2, \quad \lambda_H^2 = 0.06 \pm 0.03 \text{ GeV}^2. \quad (39)$$

The Borel parameter M^2 follows a uniform distribution within $[2, 3] \text{ GeV}^2$. We generate 50 random points from the distribution and find the values of the threshold parameters satisfying

Eq. (38) for each of the 50 combinations of the above mentioned parameters, thus leading to a distribution for the threshold parameter s_0 for the form factors f_+ and f_T for four q^2 values in the range -15 GeV^2 to 0 GeV^2 . We observe very mild q^2 dependence of the threshold parameters and the values are consistent within their corresponding $\pm 1\sigma$ confidence interval (CI). From a conservative viewpoint, we take the average of the values obtained at the four different points of q^2 as our central value for the threshold parameter and the highest uncertainty as our uncertainty estimate as given below,

$$s_0 = \begin{cases} 1.10 \pm 0.38 \text{ GeV}^2 & (f_+, f_0), \\ 1.23 \pm 0.31 \text{ GeV}^2 & (f_T). \end{cases} \quad (40)$$

We are now at a stage to estimate the form factors for $B_s \rightarrow \eta_s$ transition using the sum rules obtained in Sec. 3. We first create LCSR data points for the form factors f_+ and f_T at $q^2 = \{-15, -10, -5, 0, 5\} \text{ GeV}^2$ and for f_0 at $q^2 = \{-15, -10, -5, 5\} \text{ GeV}^2$. For the extrapolation in the semileptonic region i.e., $4m_\ell^2 < q^2 < (m_{B_s} - m_{\eta_s})^2$, we perform a $q^2 \rightarrow z$ map by fitting these data points to a series expansion in parameter z

$$z(q^2) = \frac{\sqrt{t_+ - q^2} - \sqrt{t_+ - t_0}}{\sqrt{t_+ - q^2} + \sqrt{t_+ - t_0}}, \quad (41)$$

where

$$t_+ = (m_{B_s} + m_{\eta_s})^2, \quad t_0 = (m_{B_s} + m_{\eta_s}) (\sqrt{m_{B_s}} - \sqrt{m_{\eta_s}})^2. \quad (42)$$

The form factor then can be written as

$$F_{\text{fit}}^{(i)}(q^2) = \frac{1}{1 - \frac{q^2}{m_{(i)}^2}} \sum_{k=0}^2 a_k^{(i)} [z(q^2) - z(0)]^k. \quad (43)$$

Here, $a_k^{(i)}$ are the form factor parameters⁵. The resonance mass parameters, denoting the sub-thresholds with appropriate quantum numbers, used are $m_{(0)} = 5.630 \text{ GeV}$ and $m_{(+,T)} = 5.412 \text{ GeV}$ for f_0 and $f_{+,T}$, respectively [20]. The prediction of all three form factors as a function of q^2 is shown in Fig. 3. The green band denotes the $\pm 1\sigma$ uncertainty envelope. The uncertainties of our calculation for $q^2 > 10 \text{ GeV}^2$ further increase in the semileptonic region due to the extrapolation and hence we restrict the plot only up to that point.

Our next aim is to look for improvement in the uncertainty for the form factor predictions which is dominated by the highly uncertain parameter λ_{B_s} . In this regard, we perform the numerical analysis to extract the value of λ_{B_s} using the form factor estimates at $q^2 = 0 \text{ GeV}^2$ from the HPQCD collaboration [7]. We first define an optimized χ^2 - statistic as

$$\chi^2 = \sum_{i,j} (O_i^{\text{Lattice}} - O_i^{\text{theo}}) \cdot \text{Cov}_{ij}^{-1} \cdot (O_j^{\text{Lattice}} - O_j^{\text{theo}}) + \chi_{\text{nuis}}^2. \quad (44)$$

Here, O_i^{Lattice} corresponds to the Lattice inputs (central values) of the form factors f_+ and f_T for the $B_s \rightarrow \eta_s$ transition at $q^2 = 0$ ⁶ and Cov is the corresponding covariance matrix which

⁵In this work, all the form factors are truncated at $k = 2$.

⁶Note that at $q^2 = 0$, as $f_+(0) = f_0(0)$, we do not include $f_0(0)$ in the χ^2 statistic.

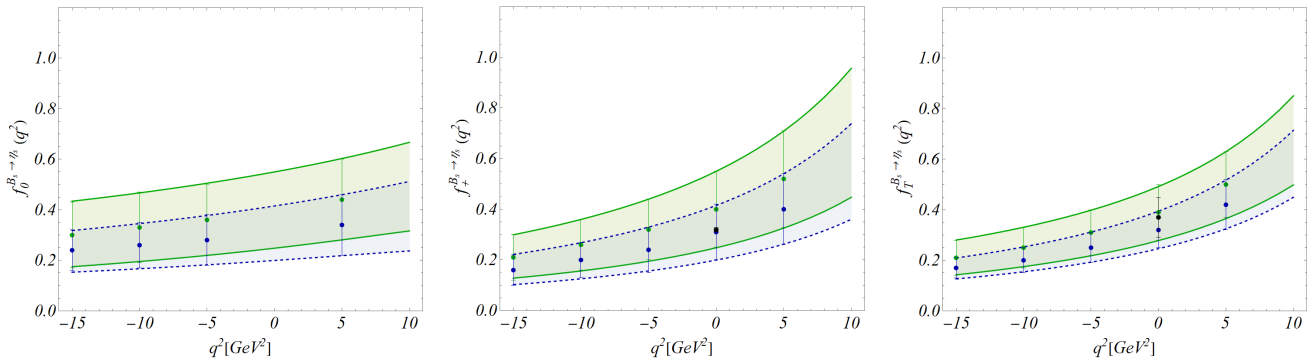


Figure 3: The variation of $B_s \rightarrow \eta_s$ form factors f_+ , f_0 and f_T as a function of momentum transfer q^2 . The green solid band with error bars represent the $\pm 1\sigma$ uncertainty envelope using QCD sum rule estimate of inverse moment parameter λ_{B_s} in Eq. (39) whereas the blue dashed band and error bars denote the prediction using the extracted value of λ_{B_s} in Eq. (45). The data points for $f_{+,T}$ at $q^2 = 0$ GeV^2 from the HPQCD collaboration [7] are also shown in black.

includes the correlation in data. We have assigned χ^2 corresponding to the nuisance parameters λ_E^2 , λ_H^2 , s_0 and M^2 in χ_{nuis}^2 where the parameters λ_E^2 , λ_H^2 and s_0 follow Gaussian distributions, as discussed above with the corresponding 1σ CIs. quoted in Eqs. (39) and (40), whereas M^2 follows a uniform distribution. Note that while determining the effective threshold s_0 in Eq. (40), the input value of λ_{B_s} is used however we mention that the procedure of taking ratio (outlined in Eq. (38)) reduces the dependency on the input parameters. Furthermore, by treating s_0 as a nuisance parameter and varying it in the χ^2 fit, this effect is further minimized. Alternatively, one conventional approach is to set the value of s_0 the same as the effective threshold obtained in the analysis of the two-point sum rule for the decay constant, as seen in Eq. (21). However, due to its significant uncertainty, we opt not to use it here.

Using the statistical frequentist procedure as described in Ref. [8], we obtain

$$\lambda_{B_s}(1 \text{ GeV}) = (480_{-83}^{+92}) \text{ MeV}. \quad (45)$$

Here, in this indirect extraction, a ‘reasonable’ choice of the factorization scale $\mu = 1 \text{ GeV}$ is assumed at which the values of other input parameters entering in the sum rule are considered.

We now compare the predictions for the form factors for $B_s \rightarrow P(P = \eta_s, K, D_s)$ channels using our estimate of λ_{B_s} with the earlier analyses. The LCSR data points are created using the analytic expression (36) for five (four) different points in the q^2 region $[-15, 5] \text{ GeV}^2$ for the form factors $f_{+,T}(f_0)$ for $B_s \rightarrow \eta_s$ and $B_s \rightarrow K$ modes, whereas for the $B_s \rightarrow D_s$ mode, we restrict ourselves till $q^2 = 0 \text{ GeV}^2$ since the relative contribution from the higher-twist two-particle terms increases with increasing positive values of q^2 making the calculation of the form factors unstable, as discussed in Ref. [18]. Subsequently we use the z -parametrization for the extrapolation of form factors from negative q^2 to the semileptonic region using Eq. (43) with appropriate mass parameters. The central values and $\pm 1\sigma$ CIs of the parameters $a_k^{(i)}$ are provided in Appendix C (Table 2), along with their correlations (Tables 3, 4 and 5). For the $B_s \rightarrow \eta_s$ channel, we now compare the form factor predictions with our previous result i.e., using λ_{B_s} value from QCD sum rule estimate in Eq. (39) in green bands with the extracted value in Eq. (45) in blue bands. All other parameters are chosen to be same as already discussed above. As expected, the form factor estimates using the λ_{B_s} value from Eq. (39) have larger uncertainties and are relatively

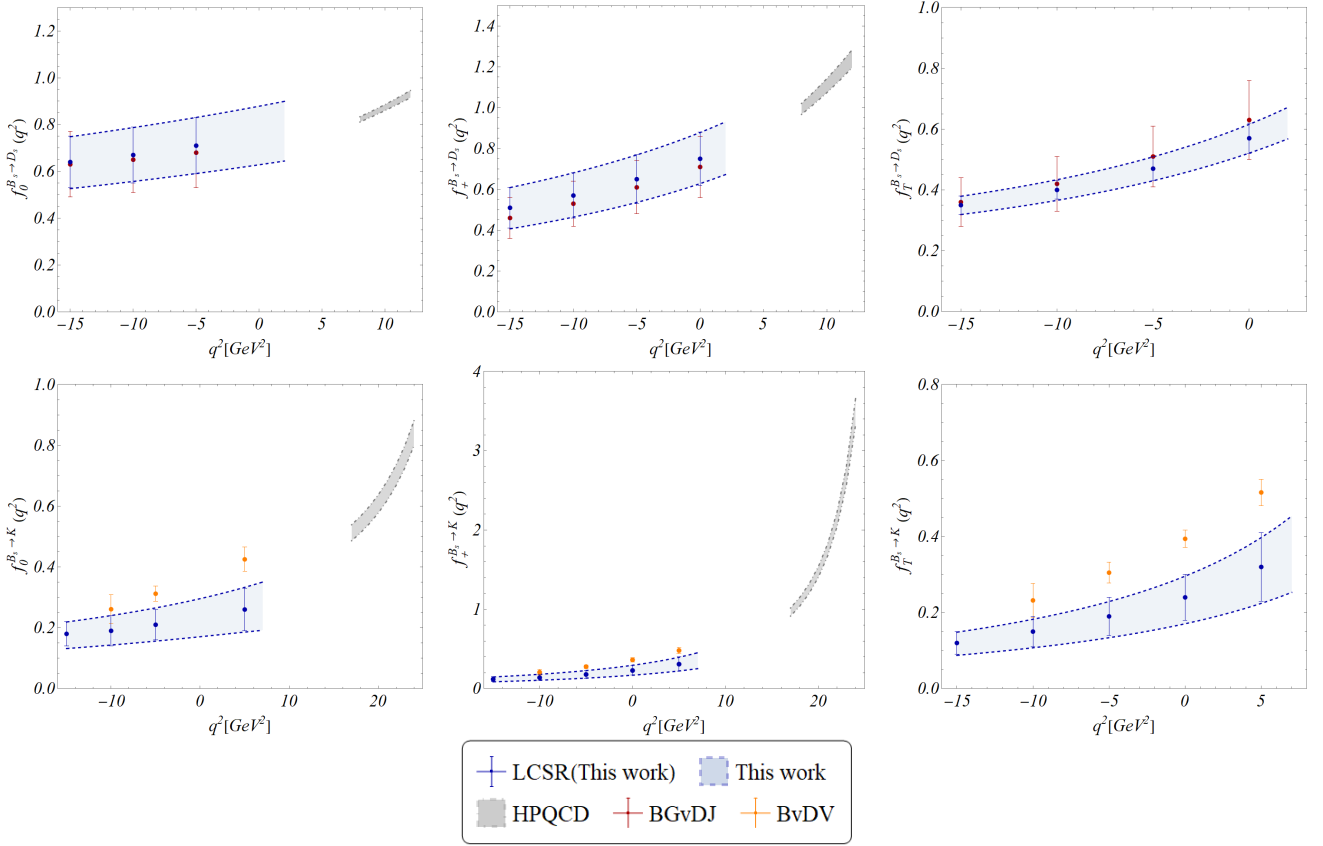


Figure 4: The variation of the form factors with momentum transfer q^2 for the modes $B_s \rightarrow D_s$ (upper row) and $B_s \rightarrow K$ (lower row). The blue band and error bars represent LCSR predictions using our extracted value of λ_{B_s} (Eq. (45)). The red(orange) error bars correspond to the LCSR estimates from BGvDJ [21](BvDV [22]). The grey bands correspond to Lattice QCD estimates from HPQCD collaboration (see Ref. [23] for $B_s \rightarrow D_s$ and Ref. [24] for $B_s \rightarrow K$ decays.)

higher as compared to the estimates using the obtained value of λ_{B_s} in our case, though the results are highly consistent with each other. We also show the data points at $q^2 = 0 \text{ GeV}^2$ from the HPQCD collaboration [7] in black, which agrees well with our estimates as expected.

For the $B_s \rightarrow D_s$ channel, we compare our results to those from Ref. [21] [BGvDJ](red error bars), where B -meson LCDAs have been used ignoring the $SU(3)_F$ violation effect due to the presence of s -quark in the meson. Considering the values of the threshold and Borel parameters from [BGvDJ], we calculate the form factors with our extracted value of λ_{B_s} . For the form factors f_0 and f_+ , the values obtained in our case are slightly higher than [BGvDJ], whereas for the f_T form factor, the pattern is opposite. For this channel also, the uncertainty for all the form factors are reduced and the results are highly consistent with each other. We have also shown Lattice QCD estimates from the HPQCD collaboration [23] for $q^2 \gtrsim 8 \text{ GeV}^2$ as the lattice simulations for this mode are most precise in this region⁷.

In the case of $B_s \rightarrow K$ channel, the predictions of form factors using B_s -meson LCDAs (with QCD sum rule estimate of λ_{B_s} in Eq. (39)) bear with large uncertainty. However, the precise prediction for form factors are obtained using K -meson LCDAs in Ref. [22] [BvDV]

⁷The Lattice QCD estimates are available only for the form factors f_+ and f_0 for the $B_s \rightarrow (K, D_s)$ modes.

and thus we compare our results to those of [BvDV] (orange error bars). We have obtained the threshold parameters separately for the form factors f_+ and f_T following the method as described above (for $B_s \rightarrow \eta_s$) resulting into $s_0 = 0.58 \pm 0.04 \text{ GeV}^2$ ($0.63 \pm 0.11 \text{ GeV}^2$) for form factors $f_+(f_T)$. We notice that the uncertainties of the form factors obtained using light-meson LCDAs is significantly reduced in comparison to our results, which is as per the expectation. We find that the central values obtained in [BvDV] are relatively higher than ours and are consistent only at 2σ CI for most of the region. These are two complementary methods to calculate the form factors and we have demonstrated that improvement in B_s -meson LCDA parameters will eventually lead to predictions with comparable uncertainty. We have also shown Lattice estimates from the HPQCD collaboration [24] for $q^2 \gtrsim 16 \text{ GeV}^2$ region for the form factors f_+ and f_0 . However, there is currently no estimate available for the form factor f_T , also from other Lattice collaborations [25, 26] in the same decay mode.

5 Summary

In this study, we utilize form factor results obtained from Lattice QCD concerning the η_s -meson. The η_s -meson, a fictitious $s\bar{s}$ bound state used to calibrate the s -quark mass in Lattice QCD analyses, is generally restricted in its application and has not been utilized elsewhere. Initially, we employ the QCD sum rule framework to compute the decay constant for the η_s -meson using two-point sum rules. Perturbative contributions are accounted for up to next-to-leading order, while condensate effects are considered up to dimension five operators. Notably, these contributions are largely proportional to the s -quark mass, except for the gluon condensate, which significantly influences the sum rule. Our prediction for the decay constant is consistent with the Lattice QCD estimate and has a smaller degree of uncertainty.

With estimates of intrinsic parameters for QCD sum rules in hand, we proceed to compute the $B_s \rightarrow \eta_s$ form factors within the LCSR framework, using B_s -meson LCDAs. These analytical expressions for the form factors are then utilized to extract the inverse moment of the leading-twist B_s -meson LCDA, denoted as λ_{B_s} , leveraging recent Lattice QCD results obtained for these form factors at zero momentum transfer ($q^2 = 0 \text{ GeV}^2$) from the HPQCD collaboration. Our analysis yields $\lambda_{B_s} = (480 \pm 92) \text{ MeV}$ when employing the Exponential model for B_s -meson LCDA parametrization. Notably, this value is consistent with prior QCD sum rule estimate of λ_{B_s} , however exhibiting a 1.5-fold reduction in uncertainty.

Using the indirectly determined value of λ_{B_s} , we proceed to compare the form factor estimates across various modes of B_s -meson decay, including $B_s \rightarrow D_s$ and $B_s \rightarrow K$. Our findings reveal consistency with previously obtained $B_s \rightarrow D_s$ form factors calculated using B -meson LCDAs, albeit with improved overall uncertainties in our analysis. However, comparisons with previous $B_s \rightarrow K$ form factor predictions, utilizing K -meson LCDAs, demonstrate significantly greater precision compared to estimates derived from B_s -meson LCDAs, despite the incorporation of the constrained value of λ_{B_s} obtained in this work.

Acknowledgement:

R.M. acknowledges SERB Grant SPG/2022/001238 for the support. I.R.'s work receives support from the IIT Gandhinagar Research and Development Grant IP/IITGN//PHY/RM/2223/11.

A B_s -meson light-cone distribution amplitudes

We express the B_s -to-vacuum matrix element in the heavy quark effective theory limit in which the heavy b -quark field is substituted with the heavy quark effective theory field h_v , with $v^\mu = (q+k)^\mu/m_{B_s}$ representing the B_s -meson's four-velocity in its rest frame. The expansion in terms of the different twists two-particle B_s -meson LCDAs is given as [27]

$$\langle 0 | \bar{s}^\alpha(x) h_v^\beta(0) | \bar{B}_s(v) \rangle = -\frac{if_{B_s} m_{B_s}}{4} \int_0^\infty d\omega \left\{ (1 + \psi) \left[\phi_+(\omega) - g_+(\omega) \partial_\lambda \partial^\lambda + \frac{1}{2} (\bar{\phi}(\omega) - \bar{g}(\omega) \partial_\lambda \partial^\lambda) \gamma^\rho \partial_\rho \right] \gamma_5 \right\}^{\beta\alpha} e^{-ir \cdot x} \Big|_{r=\omega v}. \quad (46)$$

The derivatives $\partial_\mu \equiv \partial/\partial r^\mu$ are understood to act on the hard-scattering kernel.

The Exponential model for B_s -meson LCDAs is given as [27, 28]

$$\phi_+(\omega) = \frac{\omega}{\lambda_{B_s}^2} e^{-\omega/\lambda_{B_s}}, \quad (47)$$

$$\phi_-(\omega) = \frac{1}{\lambda_{B_s}} e^{-\omega/\lambda_{B_s}} - \frac{\lambda_E^2 - \lambda_H^2}{18\lambda_{B_s}^5} (2\lambda_{B_s}^2 - 4\omega\lambda_{B_s} + \omega^2) e^{-\omega/\lambda_{B_s}}, \quad (48)$$

$$g_+(\omega) = -\frac{\lambda_E^2}{6\lambda_{B_s}^2} \left\{ (\omega - 2\lambda_{B_s}) \text{Ei} \left(-\frac{\omega}{\lambda_{B_s}} \right) + (\omega + 2\lambda_{B_s}) e^{-\omega/\lambda_{B_s}} \times \left(\ln \frac{\omega}{\lambda_{B_s}} + \gamma_E \right) - 2\omega e^{-\omega/\lambda_{B_s}} \right\} + \frac{e^{-\omega/\lambda_{B_s}}}{2\lambda_{B_s}} \omega^2 \left\{ 1 - \frac{1}{36\lambda_{B_s}^2} (\lambda_E^2 - \lambda_H^2) \right\}, \quad (49)$$

$$g_-^{WW}(\omega) = \frac{1}{4} \int_0^\omega d\eta_2 \int_0^{\eta_2} d\eta_1 [\phi_+(\eta_1) - \phi_-^{WW}(\eta_1)] - \frac{1}{2} \int_0^\omega d\eta_1 \left(\eta_1 - \frac{3}{2}\lambda_{B_s} \right) \phi_-^{WW}(\eta_1) = \frac{3\omega}{4} e^{-\omega/\lambda_{B_s}}. \quad (50)$$

where $\phi_-^{WW}(\eta_1) = e^{-\eta_1/\lambda_{B_s}}/\lambda_{B_s}$ and $\text{Ei}(x)$ is the exponential integral. The approximate expression for g_- is derived in the Wandzura-Wilczek limit, as mentioned in Ref. [18] where the three-component amplitudes are neglected (see also Ref. [29])⁸.

B Coefficients of the LCSR formula

Here, we provide a listing of all the coefficients of the two-particle LCDAs that are involved in Eq. (36). With the introduction of following notation

$$f_\pm = \frac{q^2 - m_{B_s}^2 + m_P^2}{q^2} f_+ + \frac{m_{B_s}^2 - m_P^2}{q^2} f_0, \quad (51)$$

⁸The LCDA g_- being of twist five is suppressed as compared to the leading twist LCDAs and, thus its contribution in the form factors is numerically insignificant.

we obtain, for $f_+^{B_s \rightarrow P}$:

$$\begin{aligned}
C_1^{(f_+^{B_s \rightarrow P}, \phi_+)} &= -\bar{\sigma}, \\
C_2^{(f_+^{B_s \rightarrow P}, \bar{\phi})} &= -m_{B_s} \bar{\sigma}^2, \\
C_2^{(f_+^{B_s \rightarrow P}, g_+)} &= -4\bar{\sigma}, \\
C_3^{(f_+^{B_s \rightarrow P}, g_+)} &= 8m_{q_1}^2 \bar{\sigma}, \\
C_3^{(f_+^{B_s \rightarrow P}, \bar{g})} &= -8m_{B_s} \bar{\sigma}^2, \\
C_4^{(f_+^{B_s \rightarrow P}, \bar{g})} &= 24m_{q_1}^2 m_{B_s} \bar{\sigma}^2.
\end{aligned} \tag{52}$$

For $f_{\pm}^{B_s \rightarrow P}$:

$$\begin{aligned}
C_1^{(f_{\pm}^{B_s \rightarrow P}, \phi_+)} &= 2\sigma - 1, \\
C_2^{(f_{\pm}^{B_s \rightarrow P}, \bar{\phi})} &= 2m_{B_s} \sigma \bar{\sigma} - m_{q_1}, \\
C_2^{(f_{\pm}^{B_s \rightarrow P}, g_+)} &= 4(2\sigma - 1), \\
C_3^{(f_{\pm}^{B_s \rightarrow P}, g_+)} &= -8m_{q_1}^2 (2\sigma - 1), \\
C_3^{(f_{\pm}^{B_s \rightarrow P}, \bar{g})} &= 16m_{B_s} \sigma \bar{\sigma}, \\
C_4^{(f_{\pm}^{B_s \rightarrow P}, \bar{g})} &= 24m_{q_1}^2 (m_{q_1} - 2m_{B_s} \sigma \bar{\sigma}).
\end{aligned} \tag{53}$$

For $f_T^{B_s \rightarrow P}$:

$$\begin{aligned}
C_1^{(f_T^{B_s \rightarrow P}, \bar{\phi})} &= \frac{1}{m_{B_s}}, \\
C_2^{(f_T^{B_s \rightarrow P}, \bar{\phi})} &= \frac{-(m_{B_s}^2 \bar{\sigma}^2 - m_{q_1}^2 + 2q^2 \sigma - q^2)}{m_{B_s}}, \\
C_2^{(f_T^{B_s \rightarrow P}, \bar{g})} &= \frac{8}{m_{B_s}}, \\
C_3^{(f_T^{B_s \rightarrow P}, \bar{g})} &= \frac{-8(m_{B_s}^2 \bar{\sigma}^2 + 2m_{q_1}^2 + 2q^2 \sigma - q^2)}{m_{B_s}}, \\
C_4^{(f_T^{B_s \rightarrow P}, \bar{g})} &= \frac{24m_{q_1}^2 (m_{B_s}^2 \bar{\sigma}^2 - m_{q_1}^2 + 2q^2 \sigma - q^2)}{m_{B_s}}.
\end{aligned} \tag{54}$$

The normalization factors (in Eq. (36)) are,

$$K^{(f_+^{B_s \rightarrow P})} = K^{(f_{\pm}^{B_s \rightarrow P})} = f_P, \quad K^{(f_T^{B_s \rightarrow P})} = \frac{f_P (m_{B_s}^2 - m_P^2 - q^2)}{m_{B_s} (m_{B_s} + m_P)}. \tag{55}$$

In the above expressions, the quark mass m_{q_1} enters for different transitions with $q_1 = s, d$ and c for the modes $B_s \rightarrow \eta_s, K$ and D_s , respectively.

C Fitted coefficients and the correlations

In Table 2, we present the results for the fitted expansion coefficients, denoted as $a_k^{(i)}$ in Eq. (43), for the various modes considered in this study. The respective correlations among the fitted coefficients are provided in Tables 3, 4, and 5.

| | $B_s \rightarrow \eta_s$ | $B_s \rightarrow K$ | $B_s \rightarrow D_s$ |
|---------|--------------------------|---------------------|-----------------------|
| a_0^+ | 0.31 ± 0.11 | 0.23 ± 0.06 | 0.75 ± 0.13 |
| a_1^+ | -0.71 ± 0.23 | -0.59 ± 0.21 | -0.86 ± 0.49 |
| a_2^+ | -0.31 ± 0.49 | -0.13 ± 0.35 | -0.69 ± 1.86 |
| a_1^0 | 0.56 ± 0.19 | 0.39 ± 0.04 | 2.00 ± 0.48 |
| a_2^0 | -1.03 ± 0.22 | -0.74 ± 0.05 | -1.82 ± 0.56 |
| a_0^T | 0.32 ± 0.07 | 0.24 ± 0.06 | 0.57 ± 0.05 |
| a_1^T | -0.79 ± 0.18 | -0.62 ± 0.21 | -2.03 ± 0.47 |
| a_2^T | 0.002 ± 0.48 | -0.06 ± 0.38 | 9.51 ± 2.29 |

Table 2: z -expansion coefficients for the various channels considered in this work.

| | a_0^+ | a_1^+ | a_2^+ | a_1^0 | a_2^0 | a_0^T | a_1^T | a_2^T |
|---------|---------|---------|---------|---------|---------|---------|---------|---------|
| a_0^+ | 1. | -0.89 | -0.117 | 0.885 | -0.497 | 0.1 | -0.061 | -0.005 |
| a_1^+ | -0.89 | 1. | -0.341 | -0.593 | 0.196 | -0.067 | -0.024 | 0.123 |
| a_2^+ | -0.117 | -0.341 | 1. | -0.544 | 0.691 | -0.034 | 0.155 | -0.262 |
| a_1^0 | 0.885 | -0.593 | -0.544 | 1. | -0.793 | 0.111 | -0.122 | 0.104 |
| a_2^0 | -0.497 | 0.196 | 0.691 | -0.793 | 1. | -0.064 | 0.097 | -0.143 |
| a_0^T | 0.1 | -0.067 | -0.034 | 0.111 | -0.064 | 1. | -0.83 | 0.208 |
| a_1^T | -0.061 | -0.024 | 0.155 | -0.122 | 0.097 | -0.83 | 1. | -0.693 |
| a_2^T | -0.005 | 0.123 | -0.262 | 0.104 | -0.143 | 0.208 | -0.693 | 1. |

Table 3: Correlation among the z -expansion coefficients for $B_s \rightarrow \eta_s$ mode.

References

- [1] V. M. Braun, D. Y. Ivanov, and G. P. Korchemsky, *The B meson distribution amplitude in QCD*, *Phys. Rev. D* **69** (2004) 034014, [arXiv:hep-ph/0309330](#).
- [2] A. Khodjamirian, R. Mandal, and T. Mannel, *Inverse moment of the B_s -meson distribution amplitude from QCD sum rule*, *JHEP* **10** (2020) 043, [arXiv:2008.03935](#) [[hep-ph](#)].
- [3] T. Feldmann, P. Lüghausen, and N. Seitz, *Strange-quark mass effects in the B_s meson's light-cone distribution amplitude*, *JHEP* **08** (2023) 075, [arXiv:2306.14686](#) [[hep-ph](#)].

| | a_0^+ | a_1^+ | a_2^+ | a_1^0 | a_2^0 | a_0^T | a_1^T | a_2^T |
|---------|---------|---------|---------|---------|---------|---------|---------|---------|
| a_0^+ | 1. | -0.988 | 0.88 | 0.73 | 0.243 | 0.011 | -0.013 | 0.015 |
| a_1^+ | -0.988 | 1. | -0.943 | -0.623 | -0.366 | -0.005 | 0.005 | -0.004 |
| a_2^+ | 0.88 | -0.943 | 1. | 0.342 | 0.606 | -0.011 | 0.015 | -0.022 |
| a_1^0 | 0.73 | -0.623 | 0.342 | 1. | -0.468 | 0.027 | -0.039 | 0.057 |
| a_2^0 | 0.243 | -0.366 | 0.606 | -0.468 | 1. | -0.032 | 0.045 | -0.066 |
| a_0^T | 0.011 | -0.005 | -0.011 | 0.027 | -0.032 | 1. | -0.973 | 0.793 |
| a_1^T | -0.013 | 0.005 | 0.015 | -0.039 | 0.045 | -0.973 | 1. | -0.912 |
| a_2^T | 0.015 | -0.004 | -0.022 | 0.057 | -0.066 | 0.793 | -0.912 | 1. |

Table 4: Correlation among the z -expansion coefficients for $B_s \rightarrow K$ mode.

| | a_0^+ | a_1^+ | a_2^+ | a_1^0 | a_2^0 | a_0^T | a_1^T | a_2^T |
|---------|---------|---------|---------|---------|---------|---------|---------|---------|
| a_0^+ | 1. | 0.556 | -0.673 | 0.855 | 0.153 | 0.256 | 0.698 | -0.539 |
| a_1^+ | 0.556 | 1. | -0.883 | 0.89 | 0.009 | -0.533 | 0.869 | -0.519 |
| a_2^+ | -0.673 | -0.883 | 1. | -0.887 | 0.341 | 0.246 | -0.932 | 0.805 |
| a_1^0 | 0.855 | 0.89 | -0.887 | 1. | 0.044 | -0.128 | 0.846 | -0.561 |
| a_2^0 | 0.153 | 0.009 | 0.341 | 0.044 | 1. | -0.132 | -0.113 | 0.495 |
| a_0^T | 0.256 | -0.533 | 0.246 | -0.128 | -0.132 | 1. | -0.383 | -0.002 |
| a_1^T | 0.698 | 0.869 | -0.932 | 0.846 | -0.113 | -0.383 | 1. | -0.795 |
| a_2^T | -0.539 | -0.519 | 0.805 | -0.561 | 0.495 | -0.002 | -0.795 | 1. |

Table 5: Correlation among the z -expansion coefficients for $B_s \rightarrow D_s$ mode.

- [4] M. Beneke, C. Bobeth, and Y.-M. Wang, $B_{d,s} \rightarrow \gamma \ell \bar{\ell}$ decay with an energetic photon, *JHEP* **12** (2020) 148, arXiv:2008.12494 [hep-ph].
- [5] R. J. Dowdall, C. T. H. Davies, G. P. Lepage, and C. McNeile, Vus from π and K decay constants in full lattice QCD with physical u , d , s and c quarks, *Phys. Rev. D* **88** (2013) 074504, arXiv:1303.1670 [hep-lat].
- [6] K. Azizi, R. Khosravi, and F. Falahati, Rare Semileptonic B_s Decays to η and η' mesons in QCD, *Phys. Rev. D* **82** (2010) 116001, arXiv:1008.3175 [hep-ph].
- [7] **(HPQCD collaboration)**§, HPQCD Collaboration, W. G. Parrott, C. Bouchard, and C. T. H. Davies, $B \rightarrow K$ and $D \rightarrow K$ form factors from fully relativistic lattice QCD, *Phys. Rev. D* **107** no. 1, (2023) 014510, arXiv:2207.12468 [hep-lat].
- [8] R. Mandal, S. Nandi, and I. Ray, Constraining inverse moment of B -meson distribution amplitude using Lattice QCD data, *Phys. Lett. B* **848** (2024) 138345, arXiv:2308.07033 [hep-ph].

- [9] S. C. Generalis, *QCD sum rules. 1: Perturbative results for current correlators*, *J. Phys. G* **16** (1990) 785–793.
- [10] L. J. Reinders, H. Rubinstein, and S. Yazaki, *Hadron Properties from QCD Sum Rules*, *Phys. Rept.* **127** (1985) 1.
- [11] P. Gelhausen, A. Khodjamirian, A. A. Pivovarov, and D. Rosenthal, *Radial excitations of heavy-light mesons from QCD sum rules*, *Eur. Phys. J. C* **74** no. 8, (2014) 2979, [arXiv:1404.5891](https://arxiv.org/abs/1404.5891) [hep-ph].
- [12] A. Khodjamirian, B. Melić, Y.-M. Wang, and Y.-B. Wei, *The $d^*d\pi$ and $b^*b\pi$ couplings from light-cone sum rules*, *Journal of High Energy Physics* **2021** no. 3, (Mar., 2021) . [http://dx.doi.org/10.1007/JHEP03\(2021\)016](http://dx.doi.org/10.1007/JHEP03(2021)016).
- [13] K. G. Chetyrkin, J. H. Kuhn, and M. Steinhauser, *RunDec: A Mathematica package for running and decoupling of the strong coupling and quark masses*, *Comput. Phys. Commun.* **133** (2000) 43–65, [arXiv:hep-ph/0004189](https://arxiv.org/abs/hep-ph/0004189).
- [14] **Particle Data Group** Collaboration, R. L. Workman and Others, *Review of Particle Physics*, *PTEP* **2022** (2022) 083C01.
- [15] **Flavour Lattice Averaging Group (FLAG)** Collaboration, Y. Aoki *et al.*, *FLAG Review 2021*, *Eur. Phys. J. C* **82** no. 10, (2022) 869, [arXiv:2111.09849](https://arxiv.org/abs/2111.09849) [hep-lat].
- [16] B. Ioffe, *Condensates in quantum chromodynamics*, *Physics of Atomic Nuclei* **66** (2003) 30–43.
- [17] **HPQCD Collaboration** Collaboration, W. G. Parrott, C. Bouchard, C. T. H. Davies, and D. Hatton, *Toward accurate form factors for b -to-light meson decay from lattice qcd*, *Phys. Rev. D* **103** (May, 2021) 094506. <https://link.aps.org/doi/10.1103/PhysRevD.103.094506>.
- [18] N. Gubernari, A. Kokulu, and D. van Dyk, *$B \rightarrow P$ and $B \rightarrow V$ Form Factors from B -Meson Light-Cone Sum Rules beyond Leading Twist*, *JHEP* **01** (2019) 150, [arXiv:1811.00983](https://arxiv.org/abs/1811.00983) [hep-ph].
- [19] T. Nishikawa and K. Tanaka, *QCD Sum Rules for Quark-Gluon Three-Body Components in the B Meson*, *Nucl. Phys. B* **879** (2014) 110–142, [arXiv:1109.6786](https://arxiv.org/abs/1109.6786) [hep-ph].
- [20] A. Bharucha, D. M. Straub, and R. Zwicky, *$B \rightarrow V\ell^+\ell^-$ in the Standard Model from light-cone sum rules*, *JHEP* **08** (2016) 098, [arXiv:1503.05534](https://arxiv.org/abs/1503.05534) [hep-ph].
- [21] M. Bordone, N. Gubernari, D. van Dyk, and M. Jung, *Heavy-Quark expansion for $\bar{B}_s \rightarrow D_s^{(*)}$ form factors and unitarity bounds beyond the $SU(3)_F$ limit*, *Eur. Phys. J. C* **80** no. 4, (2020) 347, [arXiv:1912.09335](https://arxiv.org/abs/1912.09335) [hep-ph].
- [22] C. Bognani, D. van Dyk, and K. K. Vos, *New determination of $|V_{ub}/V_{cb}|$ from $B_s^0 \rightarrow \{K^-, D_s^-\}\mu^+\nu$* , *JHEP* **11** (2023) 082, [arXiv:2308.04347](https://arxiv.org/abs/2308.04347) [hep-ph].

- [23] E. McLean, C. T. H. Davies, J. Koponen, and A. T. Lytle, $B_s \rightarrow D_s \ell \nu$ Form Factors for the full q^2 range from Lattice QCD with non-perturbatively normalized currents, *Phys. Rev. D* **101** no. 7, (2020) 074513, arXiv:1906.00701 [hep-lat].
- [24] C. M. Bouchard, G. P. Lepage, C. Monahan, H. Na, and J. Shigemitsu, $B_s \rightarrow K \ell \nu$ form factors from lattice QCD, *Phys. Rev. D* **90** (2014) 054506, arXiv:1406.2279 [hep-lat].
- [25] **RBC/UKQCD** Collaboration, J. M. Flynn, R. C. Hill, A. Jüttner, A. Soni, J. T. Tsang, and O. Witzel, Exclusive semileptonic $B_s \rightarrow K \ell \nu$ decays on the lattice, *Phys. Rev. D* **107** no. 11, (2023) 114512, arXiv:2303.11280 [hep-lat].
- [26] **Fermilab Lattice, MILC** Collaboration, A. Bazavov *et al.*, $B_s \rightarrow K \ell \nu$ decay from lattice QCD, *Phys. Rev. D* **100** no. 3, (2019) 034501, arXiv:1901.02561 [hep-lat].
- [27] V. M. Braun, Y. Ji, and A. N. Manashov, Higher-twist B -meson Distribution Amplitudes in HQET, *JHEP* **05** (2017) 022, arXiv:1703.02446 [hep-ph].
- [28] A. G. Grozin and M. Neubert, Asymptotics of heavy meson form-factors, *Phys. Rev. D* **55** (1997) 272–290, arXiv:hep-ph/9607366.
- [29] H. Kawamura, J. Kodaira, C.-F. Qiao, and K. Tanaka, B -meson light cone distribution amplitudes in the heavy quark limit, *Phys. Lett. B* **523** (2001) 111, arXiv:hep-ph/0109181. [Erratum: *Phys.Lett.B* 536, 344–344 (2002)].